A. BRODIN,[1] T. TURIV,[2] V. NAZARENKO[2]

[1] National Technical University of Ukraine "KPI"
(37, Peremogy Ave., Kyiv 03056, Ukraine; e-mail: alex.brodin@gmail.com)
[2] Institute of Physics, Nat. Acad. of Sci. of Ukraine
(46, Prosp. Nauky, Kyiv 03028, Ukraine)

UDC 538

ANOMALOUS DIFFUSION: SINGLE PARTICLE TRAJECTORY ANALYSIS

Single particle tracking data are usually analyzed in terms of the mean square displacement (MSD) which exhibits, in the case of Brownian particles undergoing the anomalous diffusion, a time dependence that is slower (subdiffusion) or faster (superdiffusion) than a linear one. The particle velocity autocorrelation function (VAF), which is directly related to the underlying dynamics of the host medium that brings about the anomalous diffusion, can then be obtained as the second time derivative of MSD. We examine the possibility to obtain the mean velocity autocorrelation function (MVAF) directly from the particle trace data and analyze its relation to the true VAF for an instantaneous velocity. So long as the sampling time interval is much shorter than the correlation time, MVAF gives an accurate estimate of VAF. Data analysis procedures are illustrated, by using the data generated within a simple stochastic model of superdiffusion.

Keywords: Brownian motion, anomalous diffusion, single particle tracking, mean square displacement, velocity autocorrelation function.

1. Introduction

Recent advances in single particle tracking techniques using optical video-microscopy have made it possible to examine the particle dynamics on millisecond timescales with submicrometer position errors [1–8], where deviations from the normal diffusive (Brownian) dynamics are often expected. In the simplest realization of Brownian motion, the small particles embedded in a fluid are subject to a random motion as a result of their random collisions with the surrounding particles. In the classical description of Brownian motion, developed more than a century ago [9–11], the mean displacement of a particle undergoing the Brownian motion in a Newtonian fluid is zero, whereas the mean square displacement (MSD) $\langle \Delta \mathbf{r}^2 \rangle$ increases linearly with time,

$$\langle \Delta \mathbf{r}^2(t) \rangle = 6Dt, \tag{1}$$

where $\Delta \mathbf{r}$ is the particle displacement vector over a time interval t, angle brackets denote the average over many such intervals, and D is the translational diffusion coefficient. This is the case of "normal" diffusion. Brownian particles in complex systems may, however, exhibit a quite different dynamics, reflecting the local properties of the host medium that may be inhomogeneous, exhibit a nonlinear friction, elastic properties, *etc.* Then, monitoring the thermal motion of probe particles reveals the local properties of the host medium, which is the basis of microrheology. In general, the MSD time dependence will then deviate from a linear one. Approximating the time dependence with a power law,

$$\langle \Delta \mathbf{r}^2(t) \rangle \propto t^{\alpha}, \tag{2}$$

the exponent α equals 1 in the case of normal diffusion, whereas $\alpha \neq 1$ corresponds to the superdiffusive ($\alpha > 1$) or subdiffusive ($\alpha < 1$) behavior. For instance, colloidal particles in F-actin networks, depending on their size, may exhibit a subdiffusive behavior with $0 < \alpha < 1$ [12]. Colloidal dispersions in surfactant lyotropic liquid crystals [13], in crowned polymer solutions [14], and in transient polymer networks [15], as well as proteins and lipids in cellular membranes [16], also exhibit the subdiffusion behavior with $\alpha < 1$. If the Brownian motion occurs in a system with additional degrees of freedom that exhibit a relatively slow dynamics (such as the relaxation dynamics in polymers), then this dynamics may couple to the Brownian dynamics, introducing a cer-

tain correlation into the motion of particles. For instance, the dynamics of colloidal particles in polymer networks or in a DNA polymer solution within cell cytoplasm may couple to the Rouse relaxation dynamics of the polymer and exhibit, as a result, the subdiffusive behavior with $\alpha < 1$ [17,18]. Superdiffusion with $\alpha > 1$ was observed in other kinds of polymer systems, the so-called "living polymers" [19], in dispersions of polymer-like micelles [20–22], and in concentrated suspensions of swimming bacteria [23]. Even in water, the interaction with hydrodynamic modes leads to "hydrodynamic memory" effects manifested in long negative "tails" in the particle velocity autocorrelation function [24]. So, even in normal liquids, the Brownian motion is, in fact, subdiffusive at short times. Quite recently, the anomalous sub- and superdiffusions were observed in colloidal dispersions in nematic liquid crystals [25], where they occur due to a coupling of the particle motion with the nematic liquid crystal director dynamics [25,26].

In the following, we discuss different data analysis procedures and their merits, using the model data for the superdiffusion to illustrate different approaches. We will derive the relation between the average velocity correlation function and the true instantaneous velocity correlation function and show that the former gives an accurate estimate of the latter, as long as the sampling time interval is much shorter than the correlation time.

2. Particle Trajectory Analysis

Single particle tracking using optical microscopy involves taking a series of digital images of a particle at uniformly distributed time intervals. Then the position of the particle in each image frame is determined. The resulting particle tracking data are a set of coordinates (x_i, y_i) that represent a particle trajectory at discrete instants of time $t_i = t_0 + i\Delta t$, where Δt is the sampling interval. Without any loss of generality, the time origin t_0 may be taken as zero. The amount of information contained in these data, i.e., the degree, to which the experimentally determined particle trajectory represents the real trajectory being a continuous function of time, is limited by errors $(\delta x_i, \delta y_i)$ in the position determination and the attainable time resolution Δt. Traditionally, the particle trace data are analyzed in terms of MSD *vs.* time. For a trajectory with, say, x-coordinate data $x_i = x(i\Delta t)$, $i = 0, ..., N$, MSD along x at the varying time lag $t_n = n\Delta t$ is evaluated as follows:

$$\langle \Delta x^2(t_n) \rangle = \frac{1}{N-n+1} \sum_{i=1}^{N-n+1} (x_{i+n-1} - x_{i-1})^2. \quad (3)$$

One problem within this approach is that the average in Eq. (3) is taken on overlapping and, therefore, correlated data segments. The degree of overlapping quickly increases with n, so that Eq. (3) gives a good approximation to MSD only at relatively short time lags $t_n = n\Delta t$. Next, the presence of position errors δx_i in the trace data distorts MSD, especially at short times, where MSD is small. In the simplest case of totally random δx_i, the position errors add a constant "background" to MSD [27], distorting MSD at short times, where the anomalous effects are sought.

Apart from nonlinear MSD, the anomalous diffusion can be analyzed in terms of the particle velocity autocorrelation function $C_v(t)$. Assuming that $v = v(t)$ is the instantaneous particle velocity in, say, x-direction, it is given by

$$C_v(t) = \langle v(t_0) v(t_0 + t) \rangle, \quad (4)$$

where the angular brackets mean the time average over t_0. The function $C_v(t)$ cannot be evaluated from the trace data, since the instantaneous particle velocity cannot be tracked. Meanwhile, $C_v(t)$ is related to MSD [28,29]:

$$C_v(t) = \frac{1}{2} \frac{d^2 \langle \Delta x^2(t) \rangle}{dt^2}. \quad (5)$$

Thus, the normal diffusion with $\langle \Delta x^2(t) \rangle \propto t$ corresponds to $C_v(t) = 0$, whereas $C_v(t) \neq 0$ in the case of anomalous diffusion. Specifically, $C_v(t) < 0$ corresponds to the subdiffusion, and $C_v(t) > 0$ to the superdiffusion. The function $C_v(t)$ directly reflects the underlying dynamics of the host medium that brings about the anomalous diffusion such as liquid crystal director field fluctuations in the case of a colloidal suspension in a liquid crystal [25,26]. Thus, it is the velocity correlation function rather than MSD that is the central property in the analysis of the anomalous diffusion and its models. However, taking the derivative of the (noisy) MSD data multiplies the noise and, therefore, must be accompanied by a heavy smoothing, which makes the resulting estimate of $C_v(t)$, obtained in this way, unreliable. Additionally, the (unknown) distortions of the estimated MSD, resulting

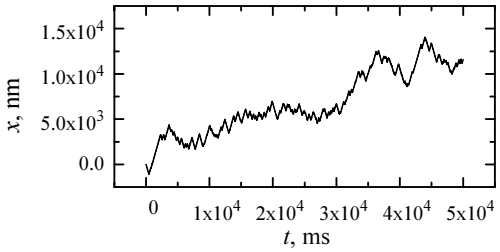

Fig. 1. Sample model trace consisting of 50,000 points

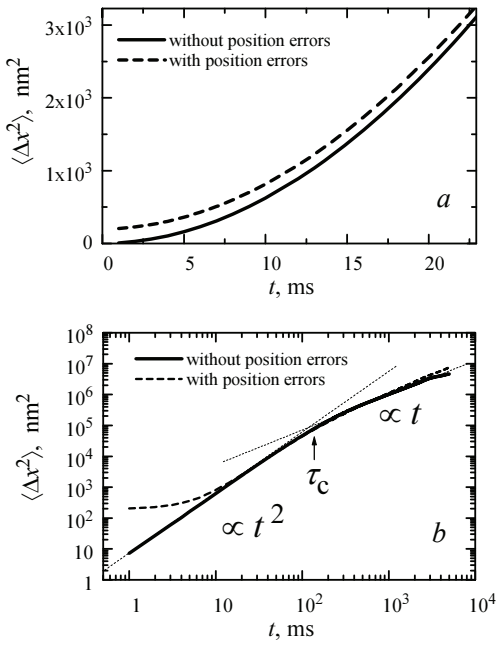

Fig. 2. MSD of simulated data traces

from overlapping and correlated segments in the average of (3), will be reflected in $C_v(t)$.

While it is not possible to evaluate the instantaneous particle velocity autocorrelation function from the trace data, as the instantaneous velocity cannot be tracked in an experiment, one can still compute the average velocity over a time interval Δt or any integer multiple thereof $n\Delta t$,

$$\bar{v}_i = \frac{x_{i+n} - x_i}{n\Delta t}, \tag{6}$$

and evaluate the *average* velocity autocorrelation function

$$C_{\bar{v}}(t_k) = \langle \bar{v}_i \bar{v}_{i+k} \rangle, \tag{7}$$

where $t_k = k\Delta t$, and the angular brackets denote the average over different i's, as was demonstrated in Ref. [25]. It is however not obvious, to which extent $C_{\bar{v}}(t)$ resembles the true $C_v(t)$.

2.1. Mean Square Displacement

Data analyses procedures will be illustrated on data for the anomalous diffusion obtained within a simple stochastic model. The model can be described as a Markov chain with one-step memory. Successive displacements Δx_i in equally spaced time intervals, Δt each, are drawn from a normal distribution $N(\mu, \sigma)$ with the mean μ and the standard deviation σ. Assuming that, at long time lags t, the diffusion is linear, i.e., $\langle \Delta x^2(t) \rangle = 2Dt$, the standard deviation is $\sigma = \sqrt{2D\Delta t}$. Each step is biased such that it is more probable to occur in the same direction as the previous step (one-step memory), resulting in the superdiffusion. Specifically, the mean μ for the step i is chosen with the same sign as the displacement in the previous step $i-1$, $\mu_i = |\mu| \, \mathrm{sign}(\Delta x_{i-1})$, with $|\mu|$ determining the superdiffusion "strength." Figure 1 shows a sample model trace data with 50,000 points, obtained with $\Delta t = 1$ ms, $D = 5 \times 10^{-14}$ m^2 s^{-1}, and $|\mu| = 2.5$ nm.

Alternatively, we simulated position determination errors δx_i, adding to each x_i a random number drawn from a normal distribution $N(0, \sigma_{\mathrm{err}})$ with $\sigma_{\mathrm{err}} = 10$ nm.

In Fig. 2, *a*, we show the initial part of MSD *versus* t, evaluated from data traces such as in Fig. 1 and computed with (dashed line) and without (solid line) position errors. It is seen that the position determination errors with $\sigma_{\mathrm{err}} = 10$ nm add a constant "background" that equals $2\sigma_{\mathrm{err}}^2 = 200$ nm^2 to MSD [27]. Figure 2, *b* presents the same data on a log-log scale.

It is seen in Fig. 2, *b* (solid line) that the simulated data exhibit the superdiffusion with $\langle \Delta x^2(t) \rangle \propto t^2$ at short times, which then goes over into the normal diffusion $\langle \Delta x^2(t) \rangle \propto t$ at time lags longer than about 150 ms. MSD for the data computed with additional position errors (dashed line) shows a spurious "plateau" at short times, which is a result of the added background. At first sight, the plateau could be interpreted as the subdiffusion, although, in fact, it is the superdiffusion, as explaned above. It is thus seen that position errors significantly distort $\langle \Delta x^2(t) \rangle$ at short times and, unless accounted for, may lead to incorrect conclusions about its shape.

Below, we proceed to discuss the velocity autocorrelation function and its evaluation from the trace data.

2.2. Velocity autocorrelation function

Let $v = v(t)$ be the instantaneous particle velocity in, say, the x-direction. We are ultimately interested in its autocorrelation function, Eq. (4). Using a shorthand pentagon notation $f \star g$ for the cross-correlation of functions $f(t)$ and $g(t)$ [30], Eq. (4) is rewritten as

$$C_v(t) = v \star v, \tag{8}$$

since the autocorrelation of a function is the cross-correlation of that function with itself.

The average velocity $\bar{v}$ over a time interval T centered at t evidently is

$$\bar{v}(t) = \frac{1}{T} \int\limits_{t-T/2}^{t+T/2} v(t')\, dt'. \tag{9}$$

Let $\Pi(t)$ be a rectangle function,

$$\Pi(t) = \begin{cases} 1 & \text{for } -T/2 \le t \le T/2; \\ 0 & \text{otherwise.} \end{cases} \tag{10}$$

Then, evidently, Eq. (9) can be recast as the convolution of $v(t)$ with $\Pi(t)$,

$$\bar{v}(t) = \frac{1}{T} \int\limits_{-\infty}^{\infty} \Pi(\tau) v(t-\tau)\, d\tau = \frac{1}{T}\, \Pi \otimes v, \tag{11}$$

where $\otimes$ is a shorthand notation for the convolution product of two functions. The autocorrelation function of $\bar{v}(t)$ is then

$$C_{\bar{v}}(t) = \bar{v} \star \bar{v} = \frac{1}{T^2}\, (\Pi \otimes v) \star (\Pi \otimes v), \tag{12}$$

where we substituted $\bar{v}$ from Eq. (11). Observing that $\Pi(t)$ is an even function, the convolution and the correlation with it are identical, $\Pi \otimes v = \Pi \star v$. Making use, furthermore, of the identity $(f \star g) \star (f \star g) = (f \star f) \star (g \star g)$ (see Appendix for its derivation), Eq. (12) is rewritten as

$$C_{\bar{v}}(t) = \frac{1}{T^2}\, (\Pi \star v) \star (\Pi \star v) = \\ = \frac{1}{T^2}\, (\Pi \star \Pi) \star (v \star v) = \Lambda(t) \star C_v(t), \tag{13}$$

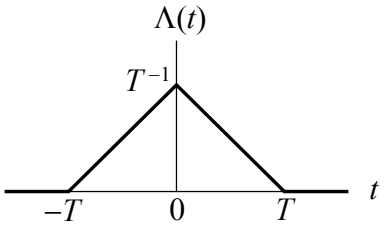

Fig. 3. Triangle function with unit area that serves as the instrumental resolution function in determining the velocity autocorrelation function from particle trace data. T is the time interval between data samples

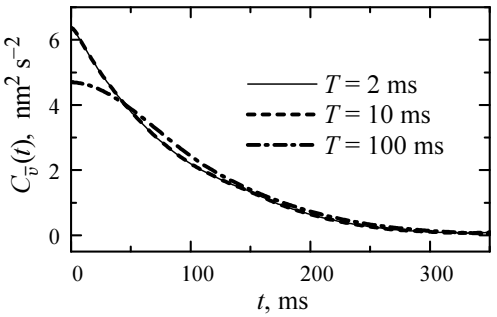

Fig. 4. Velocity autocorrelation functions obtained from the data trace of Fig. 1 (without position errors) with different averaging time intervals, as indicated

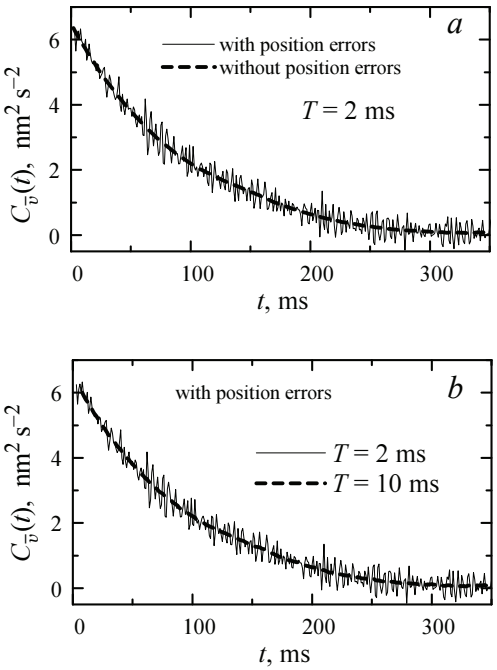

Fig. 5. Comparison of the velocity autocorrelation functions obtained from *a* datasets with and without position errors (T = = 2 ms) and *b* a dataset with position errors, with different T

where $\Lambda(t)$ is a triangle function

$$\Lambda(t) = \frac{1}{T^2}\,\Pi \star \Pi \tag{14}$$

of the width $2T$, height $1/T$, and unit area, see Fig. 3.

The autocorrelation function is an even function of time (time reversal symmetry, [31]). Since the correlation and the convolution with an even function are identical, Eq. (13) can finally be rewritten as follows:

$$C_{\bar{v}}(t) = \Lambda(t) \otimes C_v(t). \tag{15}$$

Thus, the average velocity autocorrelation function $C_{\bar{v}}(t)$, which can be evaluated from experimental particle trace data, equals the true instantaneous velocity autocorrelation function $C_v(t)$ convolved with an "instrumental resolution function" $\Lambda(t)$, whose width at half-maximum equals the averaging time interval T, which can be any integer multiple of the time interval Δt between data samples.

In Fig. 4, we compare $C_{\bar{v}}(t)$ computed from the data trace of Fig. 1 (without position errors) with different averaging intervals T.

The correlation time τ_{corr} of the functions in Fig. 4, which equals the integral of the normalized correlation function, is approximately $\tau_{\text{corr}} = 100$ ms. It is seen that the curves with $T = 2$ ms and 10 ms are almost indistinguishable. Indeed, as long as $T \ll \tau_{\text{corr}}$, i.e., the width of the instrumental function (Eq. (14), Fig. 3) is much less than the width of the correlation function, the convolution of Eq. (15) does not appreciably change the shape of $C_v(t)$. Thus, $C_{\bar{v}}(t)$ closely resembles the underlying instantaneous velocity correlation $C_v(t)$. On the contrary, the curve for $T = 100$ ms, i.e., $T \approx \tau_{\text{corr}}$, is visibly distorted.

Next, we compare $C_v(t)$ obtained with the short averaging time $T = 2$ ms from datasets with and without position errors, Fig. 5, *a*. Even though the position errors add some noise to $C_v(t)$, the shapes of the curves, apart from the noise, are the same and close to $C_v(t)$, as discussed above. In Fig. 5, *b*, we compare $C_{\bar{v}}(t)$ from the dataset with the position errors for different averaging times T.

It is seen that, at $T = 10$ ms, the noise has practically disappeared, while the corresponding correlation function is still close to the true $C_v(t)$, since $T \ll \tau_{\text{corr}}$. Thus, by analyzing the real experimental data for the anomalous diffusion, which inevitably contain the position errors, one can find an optimum averaging interval such that the noise is sufficiently suppressed, while the shape of the correlation function is not appreciably altered.

3. Conclusions

We have discussed various aspects of the analysis of single particle tracing data, specifically in systems that exhibit the anomalous diffusion at short times. Traditionally, the experimental traces are analyzed in terms of a mean square displacement, which is however distorted at short times, i.e., where anomalous effects are expected, because of the position errors in trace data. Alternatively, one can evaluate the average velocity autocorrelation function from the trace data. We show that the so obtained correlation function equals the true instantaneous velocity correlation function convolved with an "instrumental" function, whose width equals the averaging time interval. Thus, we can find an optimal averaging interval to suppress the noise in the resulting correlation function without altering its shape.

APPENDIX

Let $\mathcal{F}$ and $\mathcal{F}^{-1}$ denote the forward and inverse Fourier transforms with the usual definition [30],

$$\begin{aligned}\mathcal{F}\{f(t)\} = F(\nu) &= \int\limits_{-\infty}^{\infty} f(t)\, e^{-2\pi i\nu t}\, dt,\\ \mathcal{F}^{-1}\{F(\nu)\} = f(t) &= \int\limits_{-\infty}^{\infty} F(\nu)\, e^{2\pi i\nu t}\, d\nu.\end{aligned} \tag{A.1}$$

Let $f \star g$ denote the cross-correlation of functions $f(t)$ and $g(t)$,

$$f \star g = \int\limits_{-\infty}^{\infty} f^*(\tau) g(t+\tau)\, d\tau, \tag{A.2}$$

where f^* denotes the complex conjugate of f. Then, the cross-correlation theorem [30] states that

$$\mathcal{F}\{f \star g\} = (\mathcal{F}\{f(t)\})^* \mathcal{F}\{g(t)\}, \tag{A.3}$$

where * again denotes the complex conjugation.

Consider now the Fourier transform of the function $(f \star g) \star (f \star g)$. With the help of Eq. (A.3) and some straightforward algebra, one obtains

$$\begin{aligned}&\mathcal{F}\{(f \star g) \star (f \star g)\} = (\mathcal{F}\{(f \star g)\})^*\, \mathcal{F}\{(f \star g)\} =\\ &= ((\mathcal{F}\{f\})^* \mathcal{F}\{g\})^* (\mathcal{F}\{f\})^* \mathcal{F}\{g\} =\\ &= \mathcal{F}\{f\} (\mathcal{F}\{f\})^* (\mathcal{F}\{g\})^* \mathcal{F}\{g\} =\\ &= ((\mathcal{F}\{f\})^* \mathcal{F}\{f\})^* (\mathcal{F}\{g\})^* \mathcal{F}\{g\} =\\ &= (\mathcal{F}\{f \star f\})^* \mathcal{F}\{g \star g\} = \mathcal{F}\{(f \star f) \star (g \star g)\}.\end{aligned} \tag{A.4}$$

Thus, $\mathcal{F}\{(f\star g)\star(f\star g)\} = \mathcal{F}\{(f\star f)\star(g\star g)\}$. Performing the inverse Fourier transformation and noting that $\mathcal{F}^{-1}\{\mathcal{F}\{h\}\} = h$, one finally gets

$$(f\star g)\star(f\star g) = (f\star f)\star(g\star g). \qquad (A.5)$$

1. J. Gelles, B.J. Schnapp, and M.P. Sheetz, Nature **331**, 450 (1988).
2. J.C. Crocker and D.G. Grier, J. Colloid Interface Sci. **179**, 298 (1996).
3. P. Habdas and E.R. Weeks, Curr. Opin. Colloid Interface Sci. **7**, 196 (2002).
4. A. Pertsinidis, Y. Zhang, and S. Chu, Nature **466**, 647 (2010).
5. O. Otto, F. Czerwinski, J.L. Gornall, G. Stober, L.B. Oddershede, R. Seidel, and U.F. Keyser, Opt. Express **18**, 22722 (2010).
6. C.D. Saunter, Biophys. J. **98**, 1566 (2010).
7. E. Toprak, C. Kural, and P.R. Selvin, Methods Enzymol. **475**, 1 (2010).
8. O. Otto, J.L. Gornall, G. Stober, F. Czerwinski, R. Seidel, and U.F. Keyser, J. Opt. **13**, 044011 (2011).
9. A. Einstein, Ann. Phys. (Leipzig) **17**, 549 (1905).
10. M. von Smoluchowski, Ann. Phys. (Leipzig) **21**, 756 (1906).
11. P. Langevin, C. R. Acad. Sci. (Paris) **146**, 530 (1908).
12. I.Y. Wong, M.L. Gardel, D.R. Reichman, E.R. Weeks, M.T. Valentine, A.R. Bausch, and D.A. Weitz, Phys. Rev. Lett. **92**, 178101 (2004).
13. M.M. Alam and R. Mezzenga, Langmuir **27**, 6171 (2011).
14. D.S. Banks and C.Fradin, Biophys. J. **89**, 2960 (2005).
15. J. Sprakel, J. van der Gucht, M.A.C. Stuart, and N.A.M. Besseling, Phys. Rev. E **77**, 061502 (2008).
16. T.V. Ratto and M.L. Longo, Langmuir **19**, 1788 (2003).
17. J. Sprakel, J. van der Gucht, M. A. C. Stuart, and N. A. M. Besseling, Phys. Rev. Lett. **99**, 208301 (2007).
18. S.C. Weber, A.J. Spakowitz, and J.A. Theriot, Phys. Rev. Lett. **104**, 238102 (2010).
19. A. Ott, J.P. Bouchaud, D. Langevin, and W. Urbach, Phys. Rev. Lett. **65**, 2201 (1990).
20. Y. Gambin, G. Massiera, L. Ramos, C. Ligoure, and W. Urbach, Phys. Rev. Lett. **94**, 110602 (2005).
21. R. Ganapathy, A.K. Sood, and S. Ramaswamy, Europhys. Lett. **77**, 18007 (2007).
22. R. Angelico, A. Ceglie, U. Olsson, G. Palazzo, and L. Ambrosone, Phys. Rev. E **74**, 031403 (2006).
23. X.-L. Wu and A. Libchaber, Phys. Rev. Lett. **84**, 3017 (2000); *Ibid.* **86**, 557 (2001).
24. G.L. Paul and P.N. Pusey, J. Phys. A: Math. Gen. **14**, 3301 (1981).
25. T. Turiv, I. Lazo, A. Brodin, B.I. Lev, V. Reiffenrath, V.G. Nazarenko, and O.D. Lavrentovich, Science **342**, 1351 (2013).
26. A. Brodin, Ukr. J. Phys. **58**, 237 (2013).
27. X. Michalet, Phys. Rev. E **82**, 041914 (2010).
28. H. Scher and M. Lax, Phys. Rev. B **7**, 4491 (1973).
29. V.M. Kenkre, R. Kühne, and P. Reineker, Z. Phys. B **41**, 177 (1981).
30. R. Bracewell, *The Fourier Transform and Its Applications* (McGraw-Hill, New York, 1965).
31. L.E. Reichel, *A Modern Course in Statistical Physics* (Wiley, New York, 1998).

Received 23.03.14

О. Бродин, Т. Турів, В. Назаренко

АНОМАЛЬНА ДИФУЗІЯ:
АНАЛІЗ ТРАЄКТОРІЇ КОЛОЇДНОЇ ЧАСТИНКИ

Р е з ю м е

В ході аналізу даних з дифузії колоїдних частинок, зазвичай, розраховується середнє значення квадрата зміщення частинки, що, у випадку аномальної дифузії броунівської частинки, зростає з часом повільніше (субдифузія) або швидше (супердифузія) в порівнянні з лінійною залежністю. Автокореляційна функція швидкості частинки, яка є безпосередньо зв'язаною з динамікою середовища, що приводить до аномальної дифузії, може бути отримана як друга похідна по часу від середнього квадрата зміщення. Ми показуємо, що автокореляційна функція середньої швидкості, отримана безпосередньо з траєкторії частинки, дає достатньо точну оцінку автокореляційної функції миттєвої швидкості частинки, якщо часовий інтервал дискретизації даних є набагато коротшим за час кореляції. Чисельний аналіз проілюстровано на даних, отриманих із простої стохастичної моделі для супердифузії.

А. Бродин, Т. Турив, В. Назаренко

АНОМАЛЬНАЯ ДИФФУЗИЯ:
АНАЛИЗ ТРАЕКТОРИИ КОЛЛОИДНОЙ ЧАСТИЦЫ

Р е з ю м е

В ходе анализа данных по диффузии коллоидных частиц, как правило, рассчитывается среднее значение квадрата смещения частицы, которое, в случае аномальной диффузии броуновской частицы, растет со временем медленнее (субдиффузия) или быстрее (супердиффузия) по сравнению с линейной зависимостью. Автокорреляционная функция скорости частицы, непосредственно связанная с динамикой среды, которая приводит к аномальной диффузии, может быть получена как вторая производная по времени от среднего квадрата смещения. Мы показываем, что автокорреляционная функция средней скорости, полученная непосредственно из траектории частицы, дает достаточно точную оценку автокорреляционной функции мгновенной скорости частицы, если временной интервал дискретизации данных намного короче времени корреляции. Численный анализ проиллюстрирован на данных, полученных из простой стохастической модели для супердиффузии.